available at www.sciencedirect.com

ScienceDirect

journal homepage: www.ejconline.com

Stat3 activation is required for the growth of U87 cell-derived tumours in mice

Atreyi Dasgupta[a], *Baisakhi Raychaudhuri*[b], *Talat Haqqi*[b], *Richard Prayson*[c], *Erwin G. Van Meir*[d], *Michael Vogelbaum*[b,e], *Saikh Jaharul Haque*[a,b,*]

[a]*Department of Cancer Biology, NB-40, Lerner Research Institute, Cleveland Clinic, 9500 Euclid Avenue, Cleveland, OH 44195, USA*
[b]*Brain Tumor and Neuro-Oncology Center, Cleveland Clinic, 9500 Euclid Avenue, Cleveland, OH 44195, USA*
[c]*Department of Anatomic Pathology, Cleveland Clinic, 9500 Euclid Avenue, Cleveland, OH 44195, USA*
[d]*Department of Neurosurgery, Hematology/Oncology and Winship Cancer Institute, Emory University, Atlanta, GA 30322, USA*
[e]*Department of Neurosurgery, Cleveland Clinic, 9500 Euclid Avenue, Cleveland, OH 44195, USA*

ARTICLE INFO

Article history:
Received 10 July 2008
Received in revised form 31 October 2008
Accepted 10 November 2008
Available online 31 December 2008

Keywords:
Apoptosis
Angiogenesis
Glioblastoma multiforme
Hypoxia
Stat3
VEGF

ABSTRACT

Previously we reported that Stat3 is persistently activated in GBM tumours and derived cell lines. Hypoxia, necrosis and neo-angiogenesis are hallmarks of GBM. To unfold the contribution of activated Stat3 to the growth of GBM, we generated human GBM cell line (U87)-derived stable clones expressing a dominant negative mutant (DN)-Stat3 in a hypoxia-inducible manner, and examined their tumour-forming potentials in immune-compromised mice. We found that the parental and vector control cell-derived tumours grew steadily, whereas DN-Stat3-expressing clone-derived tumours failed to grow beyond 2 mm of thickness in mouse flanks. This blockade of tumour growth was associated with induction of tumour cell apoptosis and suppression of tumour angiogenesis. Consistent with this, mice bearing orthotopically implanted DN-Stat3-expressing clones survived significantly longer than the control mice. These data suggest that activated Stat3 is required for the growth of GBM, and that targeting Stat3 may intervene with the growth of GBM.

1. Introduction

Glioblastoma multiforme (GBM) is the most common and aggressive primary tumour of the central nervous system, with a median survival of less than a year, despite the use of surgery, radiotherapy and chemotherapy.[1,2] Primary GBM develops *de novo*, whereas the secondary GBM progresses from low-grade gliomas.[1,3,4] Secondary GBM is associated with an accumulation of molecular alterations that occur in the low-grade precursor, which include overactivation of PDGFR, amplification of CDK4 and inactivation of p53, Rb, p16/ARF and PTEN, along with an acquisition of gain-of-function mutation and amplification of the *EGFR* gene.[1,4] While deregulated EGFR signalling is detected in 45% of GBM, and loss-of-function of p53, PTEN, p16 and ARF in 55%, 36%, 52% and 49% of GBM, respectively,[5,6] constitutively active Stat3 is persistent in 94% of GBM tumours and all GBM cell lines examined.[7–9] Stat3 is expressed in latent form in all cell types, and is activated by the phosphorylation of tyrosine$_{705}$ (which is often accompanied by phosphorylation of serine$_{727}$) in cells stimulated with a variety of cytokines (IL-6, IL-11, LIF, OSM, CNTF and CT-1) and growth factors (EGF, TGF-α, PDGF and HGF).[10–12] In GBM cells, Stat3 becomes activated through multiple, aberrantly activated signalling pathways, and upregulates

* *Corresponding author:* Address: Department of Cancer Biology, NB-40, Lerner Research Institute, Cleveland Clinic, 9500 Euclid Avenue, Cleveland, OH 44195, USA. Tel.: +1 (216) 445 6622; fax: +1 (216) 445 6269.
E-mail address: haquej@ccf.org (S.J. Haque).
0959-8049/$ - see front matter
doi:10.1016/j.ejca.2008.11.027

the expression of the *bcl-2* family genes including *bcl-2* itself, *bcl-x* and *mcl-1*, resulting in the suppression of spontaneous apoptosis.[7–9]

GBM is pathologically distinct from the low-grade gliomas by virtue of its association with necrosis and neo-angiogenesis.[13,14] These findings, which are pathognomic of GBM, indicate the presence of regional tumour hypoxia as a cardinal feature of the disease.[13] The growth of GBM, as well as other solid tumours beyond 2 mm in diameter (or thickness), requires new blood vessel formation for oxygen and nutrient supply.[15–17] During hypoxia, the heterodimeric transcription factor HIF-1 or HIF-2 binds to hypoxia-responsive element (HRE) located in the regulatory regions of hypoxia-responsive genes.[18] In hypoxic GBM cells, HRE-bound HIF-1, in cooperation with other transcription factors and/or transcriptional co-activators, activates the transcription of genes encoding pro-angiogenic factors such as VEGF and IL-8.[19] Activated Stat3 has recently been shown to cooperate with HIF-1 in hypoxia-induced transcription of the *VEGF* gene in renal cell carcinoma.[20] Also, constitutively active Stat3 is shown to induce angiogenesis in melanoma cell-derived tumours grown in rodents.[21]

We hypothesise that the expression of a dominant negative mutant Stat3 (DN-Stat3)[22] in hypoxic GBM cells will induce apoptosis, and thereby block Stat3-driven pro-tumourigenic signalling required for the progression of the tumour growth. To test this hypothesis, we used a hypoxia-inducible vector to express DN-Stat3 in the tumourigenic human GBM cell line U87, and examined its tumour-forming potentials in immune-compromised *nu/nu* mice. The expression of DN-Stat3 resulted in the dormancy of U87-derived tumours in mice by reducing cell proliferation, promoting cell death (apoptosis and necrosis) and blocking neo-angiogenesis which is likely mediated by the inhibition of *VEGF* transcription in U87 cells.

2. Materials and methods

2.1. Reagents

Anti-V5 (Invitrogen, R960-25), anti-V5-FITC (Invitrogen, R963-25), anti-β-actin (Santa Cruz, SC-1615), anti-CD105 (BD Biosciences, 550546), anti-Ki-67 (DAKO, M724029), anti-phospho-Stat3 (Cell Signalling, 9131) and anti-HIF-1α (Novus, NB100-449SS) antibodies were used. TUNEL assay (ApopTag plus peroxidase in situ apoptosis) kit (Chemicon, S7101) and CSA peroxidase kit (DAKO, K1500) were used on tumour sections.

2.2. Construction of DN-Stat3 expression vector

Human Stat3 cDNA obtained from Robert Arceci (Johns Hopkins, Baltimore, MD, USA) was used as a template for site-directed mutagenesis to generate the DN-Stat3 construct, using the Quick Change XL Site-Directed Mutagenesis Kit (Stratagene, La Jolla, CA, USA) following the manufacturer's instructions. The dominant negative mutation (tyrosine$_{705}$ to phenylalanine)[22] was confirmed by nucleotide sequencing. DN-Stat3 was cloned into pcDNA-V5/HisA, and subsequently, the V5/Hisx6 tag containing DN-Stat3 was cloned in the Not I site of the hypoxia/hypoxia-inducible factor-responsive expression vector pBI-V6L that contains six tandem repeats of hypoxia response element (HRE) derived from the human *VEGF* promoter.[23] The HRE repeats were located upstream of two minimal CMV promoters driving the transcription in both the left and right orientations.[23]

2.3. Cell culture and transfection

Human embryonic kidney cell line 293T and U87 cells were grown in DMEM supplemented with 10% FBS, Penicillin (200 U/ml) and Streptomycin (200 μg/ml). To induce the expression of DN-Stat3, cells were exposed to either 1.4% O_2 or 200 μM $CoCl_2$ in 5% FBS containing low glucose (1.0 g glucose/L) media for indicated periods of time.

Transient transfection of DNA into 293T cells was performed using calcium phosphate precipitation method.[24] For generation of stable clones, U87 cells were transfected using Lipofectamine 2000 (Invitrogen), following the manufacturer's protocol. Clones were selected by culturing them in the presence of 0.5 μg/ml of puromycin for 14 days, and were expanded individually for further analyses.

2.4. Electrophorectic mobility shift assay (EMSA), Western blot analyses and luciferase assay

For EMSA, 10 μg of proteins of whole cell extracts (WCEs) and 0.2 ng of radiolabelled hSIE oligonucleotide probe were used as described.[25] Fifty micrograms of proteins were used for Western blot analysis. Luciferase reporter activity was determined and normalised as described.[24,25]

2.5. Extraction of RNA and real-time PCR

Cells were transfected with DN-Stat3 expression plasmid and were exposed to hypoxia as indicated. RNA was isolated using Trizol reagent (Invitrogen, Carlsbad, CA) according to the manufacturer's protocol. Real-time quantitative PCRs were performed to quantify *VEGF* mRNA by means of SYBR green detection and ABI 7500 Real-time PCR system (Applied Biosystems, Foster City, CA). Expression of *VEGF* relative to β-actin was analysed using the ΔC_T method using a reference gene by normalising the C_T values of the target gene (*VEGF*) to the corresponding C_T value of the control (β-actin), and expression was represented by the ratio = expression under experimental condition/normal basal expression.

2.6. Tumour implantation

Parental, vector control or DN-Stat3-expressing U87 clones (3×10^6 cells in 100 μl PBS) were mixed with matrigel (1:5) and injected (subcutaneous) into right flanks of 4-week-old male nude (*nu/nu*) athymic mice (Charles River, National Cancer Institute). Tumour volumes were measured on a weekly basis using the formula: volume = width^2 × length × 0.4.[26] To plot the survival time periods, mice were stereotactically implanted with 3×10^5 cells in 3 μl PBS in the right frontal lobe, and the Kaplan–Meier method was used. All animal experiments were conducted in accordance with the approved protocol of the Institutional Animal Care and Use Committee.

2.7. *Tissue staining, immunohistochemistry and immunocytochemistry*

After mice were sacrificed, tumours were excised and fixed in formalin or frozen with embedding media. Formalin-fixed, paraffin-embedded xenograft tumour tissue was used for haematoxylin and eosin staining, TUNEL assay and Ki-67 staining. Tissue sections were de-paraffinised and antigen retrieval was done with citrate buffer, pH 6.0. A Ventana ES-automated stainer was used to stain the sections with anti Ki-67 antibody (1:50 dilution), and stain was developed by Biotin-Avidin detection system with DAB chromogen followed by counterstaining with haematoxylin. TUNEL assay was performed according to the manufacturer's protocol. For TUNEL quantification, three fields were randomly chosen from sections of tumours after 2 weeks of tumour implantation, using a Leica DM 2000 microscope with a 40× objective lens. TUNEL-positive cells were counted as a percentage of the total cells.

DN-Stat3-V5 staining in tumour sections was performed on frozen tumour sections with V5-FITC antibody (1:500). CD105 staining was performed on frozen sections (5 μm) with 100 μl of primary antibody (1:50 dilution). Stain was developed with Alexa Fluor 595. DN-Stat3-V5 and HIF-1α stainings were performed in cells grown on coverslips in low glucose low serum media for 48 h either in the presence or in the absence of 200 μM $CoCl_2$. Cells were then fixed with 4% paraformaldehyde for 20 min. For DN-Stat3-V5, V5-FITC and for HIF-1α stainings, anti-HIF-1α antibodies were diluted at 1:500 and 1:2000, respectively. Secondary antibody attached to Alexa Fluor 568 was used to visualise HIF-1α. All sections were mounted with Vectashield containing DAPI.

3. Results

3.1. *Generation of stable U87 clones with hypoxia-inducible expression of DN-Stat3*

We employed a hypoxia-inducible vector to express DN-Stat3 for ablating the persistent activation of endogenous Stat3 in hypoxic GBM cells. First, human DN-Stat3[22] was cloned into the vector pBI-V6L[23] to generate hypoxia-regulated DN-Stat3 expression vector pBI-V6L-DN-Stat3 (Fig. 1A). The open reading frame of the DN-Stat3 was tagged with V5-epitope at the C-terminus. Expression and functionality of the pBI-V6L-DN-Stat3 construct were confirmed by transient expression in 293T cells followed by Western blot analysis using anti-V5 antibody, and by EMSA using the hSIE (human *sis*-inducible element) derived from the *c-fos* promoter, as described earlier[7,9] (data not shown). The construct was co-transfected with pBabepuro into the tumourigenic GBM cell line U87. Four clones were selected under puromycin, designated as N705, N709, N714 and N716, which showed tight DN-Stat3 regulation by hypoxia, and were used for further studies. Fig. 1B depicts a Western blot analysis, using anti-V5 antibody, of a positive (N714) and a negative (N715) clone expressing V5-tagged DN-Stat3 when exposed to hypoxia (1.4% O_2) for 24 h in two different cell culture media (4.5 g/l glucose plus 10% serum and 1.0 g/l glucose plus 5% serum). Under hypoxia, N705 and N709 clones induced DN-Stat3 levels comparable with that of N714, whereas N716 induced significantly less

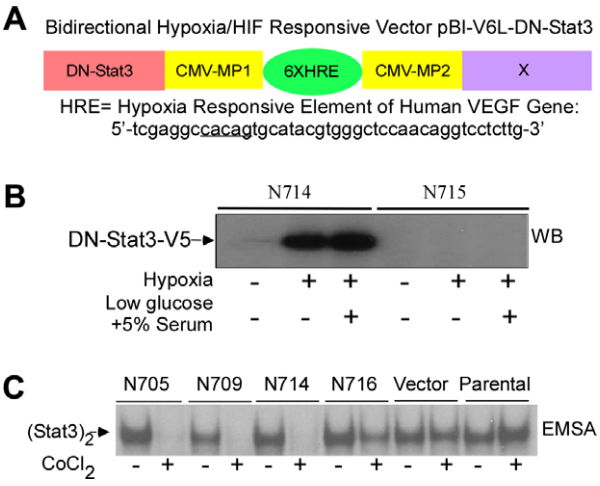

Fig. 1 – Generation of stable U87 clones with hypoxia-inducible expression of DN-Stat3. (A) Bidirectional hypoxia/HIF-responsive expression vector contains two minimal CVM promoters (CMV-MP1 and CMV-MP2) flanked by six copies of the hypoxia-responsive element (HRE) (underlined) of the human *VEGF* promoter placed either in left (pBI-V6L) or in right (pBI-V6R) orientations. DN-Stat3 cloned in the Not I site is driven by CMV-MP1. (B) One representative positive clone, N714, and a negative one, N715, were grown in DMEM (4.5 g glucose/l) plus 10% serum and in low glucose medium (1.0 g glucose/l) plus 5% serum, and exposed to hypoxia (1.4% O_2) for 24 h. Fifty micrograms of proteins in each lane were subjected to Western blot analysis using anti-V5 antibody. (C) N705, N709, N714, N716, vector control (puromycin selected pool of 20 colonies) and parental U87 cells were exposed to 200 μM $CoCl_2$ (mimics hypoxia) for 24 h and derived whole cell extracts were subjected to electrophoretic mobility shift assay (EMSA) using hSIE probe.

DN-Stat3 (data not shown). Next, we examined the DNA-binding activity of constitutively activated endogenous Stat3 by EMSA in selected clones. Whole cell extracts derived from $CoCl_2$-treated (and untreated) clones were subjected to EMSA using the hSIE probe.[7,9] The EMSA data revealed that hypoxia mimicking $CoCl_2$[27] completely ablated the DNA-binding activity of endogenous Stat3 in N705, N709 and N714, whereas in N716, the endogenous Stat3 activation was partly compromised by $CoCl_2$ or under hypoxia of 1.4% O_2 (Fig. 1C and data not shown). These results indicate that hypoxia-inducible expression of DN-Stat3 blocks the DNA-binding function of persistently activated endogenous Stat3 in U87 cells.

3.2. *Inhibition of tumour progression by hypoxia-inducible expression of DN-Stat3*

To determine the effects of hypoxia-inducible expression of DN-Stat3 on U87 clone-derived tumour growth, we implanted all four individual DN-Stat3-expressing clones in flanks of immune-compromised mice, and measured tumour volumes weekly (Fig. 2). Palpable tumours were formed by control and all DN-Stat3-expressing clones within 2 weeks of implantation. After the second week, the control groups (comprising parental U87 cells and vector control U87 cells) showed rapid

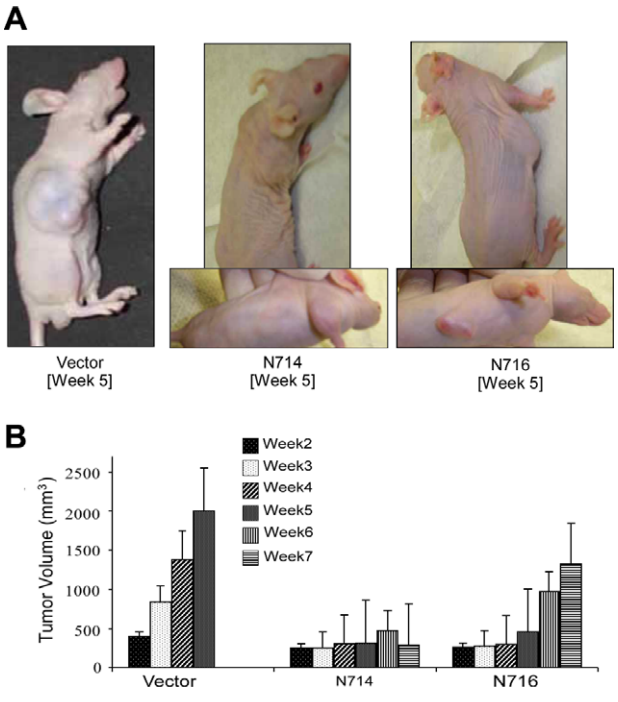

Fig. 2 – Comparison of growth of tumours derived from DN-Stat3-expressing clones (N714 and N716) and vector control U87 cell line. U87 cells (3×10^6) (vector control or DN-Stat3 clones) in a final volume of 100 μl PBS were mixed with matrigel (1:5) and injected (subcutaneous) into right flanks of 4-week-old male nude mice. Tumour volumes were determined weekly using the formula: volume = width^2 × length × 0.4 (mm^3). (A) Pictures of tumour-bearing mice at week 5. (B) Kinetics of tumour growth. Each value represents mean ± SEM of 6 individual mice in each group.

and steady growth rates, whereas the growth of tumours derived from N705, N709 and N714 clones was stagnant over 6 weeks (until the experiment was terminated) (Fig. 2B and data not shown). Interestingly, the growth of N716 (that expressed relatively low level of DN-Stat3 and thereby partly blocked the activation of endogenous Stat3)-derived tumours was dormant for 5 weeks and thereafter the tumours resumed a rapid progression of growth similar to that of control cell-derived tumours (Fig. 2B), exhibiting a DN-Stat3-dose-dependent effect on the tumour growth. It is noteworthy that tumours from the control groups grew in all dimensions, forming massive lumps, whereas small, dormant tumours derived from N705, N709 and N714 clones were flat and of not more than 2 mm in thickness showing features of growth that co-opted blood vessels just below the skin (Fig. 2A and data not shown).

Co-expression of HIF-1α and DN-Stat3-V5 was detected by immunostaining N714 cells (Fig. 3A) in the presence of 200 μM $CoCl_2$, which mimics hypoxia. Little or no expression of DN-Stat3-V5 was observed under normoxia in these cells. Under hypoxia, HIF-1α was predominantly located in nuclei, while only very little, if any, cytoplasmic expression was detected under normoxia. DN-Stat3-V5 expression was limited to the cytoplasm. Similar observations were made with N705 and N709 cells (data not shown). No expression of DN-Stat3-V5 was observed in the vector control cells grown under either hypoxia or normoxia. Tissue sections from representative tumours showed discrete regions of DN-Stat3 expression, as visualised by V5-FITC immunostaining (Fig. 3B). Localised expression of DN-Stat3 observed was likely limited to regions of hypoxia. Whereas hypoxic regions were easily discernible in the tissue sections of control group-derived tumours, they were much harder to be found in the DN-Stat3-expressing tumours. This was likely due to the fact that after hypoxia set in, the cells in those regions of the tumours started dying. This interpretation was supported by positive staining of HIF-1α in control tumours but not in DN-Stat3-expressing tumours (data not shown). Histological characteristics of the control versus DN-Stat3-expressing U87 clone-derived tumours were also strikingly different, as evident from haematoxylin-eosin staining (Supplementary Fig. 1). Dense cellular distributions that could be observed in sections derived from control U87 cell-derived tumours were strikingly absent in the DN-Stat3-expressing tumours. The latter group also exhibited more necrotic tissues compared with the control group (Supplementary Fig. 1).

3.3. *Reduced proliferation and enhanced cell death in tumours expressing DN-Stat3*

Proliferative activity of cells in tumours derived from vector control (VC) cells and the DN-Stat3-expressing clones was assessed by staining tumour sections with a monoclonal Ki-67 antibody. Overall, there were more Ki-67-positive cells in the vector- and parental cell-derived tumour tissues compared with DN-Stat3-expressing ones (Fig. 4A and data not shown). This characteristic was observed from weeks 2 to 5, after which the experiment was terminated. DN-Stat3-expressing clone-derived tumours had heterogenous distribution of Ki-67 stained cells with much fewer proliferative cells at the central regions than at the edges of the tumours, whereas the staining was more or less uniform for the control group. Cell death, more specifically apoptosis, on the other hand, was more prominent in the DN-Stat3-expressing clone-derived tumour sections, as assessed by TUNEL staining (Fig. 4B). Quantification of TUNEL-positive cells (from three random fields of each tumour section) showed significant difference between the control group and the DN-Stat3-expressing group (Fig. 4C). Whereas the control group had less than 5% apoptotic cells, the DN-Stat3-expressing tumours showed the presence of 40–80% apoptotic cells. Moreover, necrotic cells were much more abundant in DN-Stat3-expressing tumours in the later weeks than in the earlier ones, as revealed by diffuse TUNEL staining (Supplementary Fig. 2).

3.4. *Expression of DN-Stat3 prolongs the survival of tumour-bearing mice*

To confirm the role of activated Stat3 in the tumourigenicity of U87 cells *in vivo*, immune-compromised mice were implanted orthotopically with U87 cells of control (both parental and vector) and DN-Stat3-expressing (N709, N714 and N716) groups in two independent experiments (Fig. 5A and B). Both experiments clearly showed a longer survival of mice expressing hypoxia-induced DN-Stat3. While ~80% of the

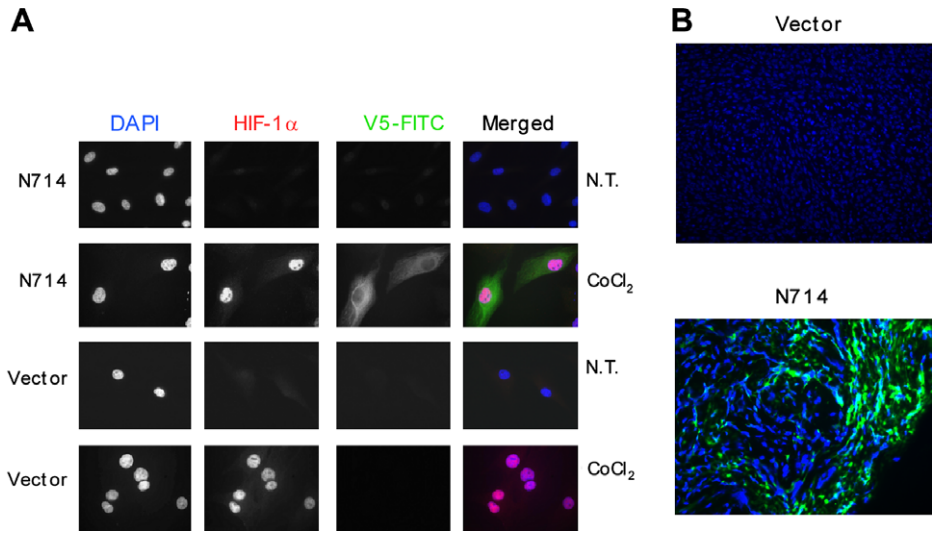

Fig. 3 – Immunostaining for HIF-1α and DN-Stat3 in cultured cells and in DN-Stat3-derived tumours. (A) N714 cells were grown on coverslips and exposed to 200 μM $CoCl_2$ for 48 h. Expression of DN-Stat3-V5 was observed under these conditions as green fluorescent staining by anti-V5-FITC, whereas nuclear staining of HIF-1α was detected by anti-HIF-1α (red fluorescence). Merged images are shown on the right. DAPI (blue) was used to stain nuclei. NT indicates no treatment. (B) Frozen tumour sections were fixed with ice-cold acetone. Fixed cells and tumour sections were permeabilised with PBS containing 0.3% Triron-X-100 and 3% serum, and incubated with FITC-conjugated anti-V5 antibody, washed and mounted with Vectashield containing DAPI. Discrete green fluorescent regions indicate V5 staining in the N714 clone-derived tumours. No non-specific staining was observed in either tissues from vector tumour or a no-antibody control (data not shown).

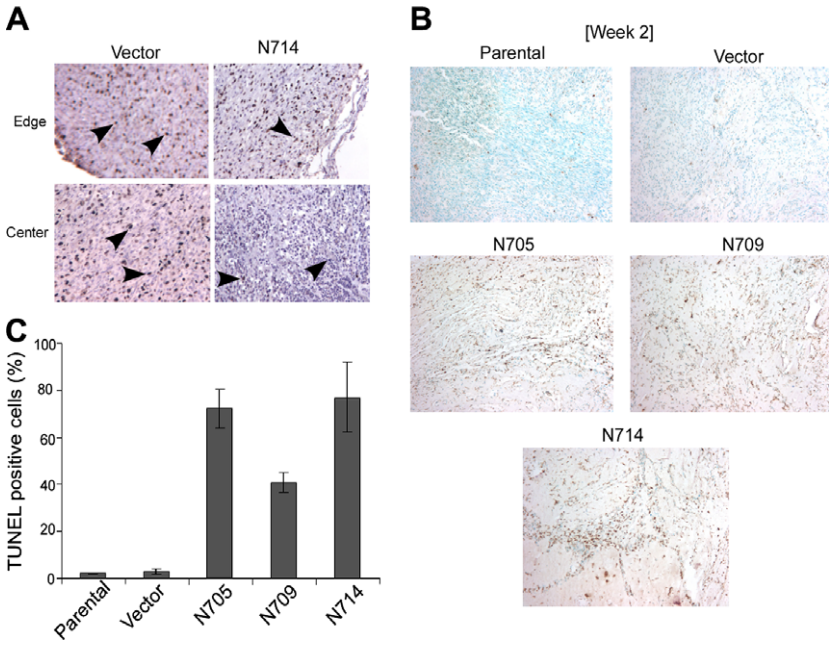

Fig. 4 – DN-Stat3 reduces tumour cell proliferation and induces apoptosis. (A) Immunohistochemical staining for Ki-67 was conducted in the paraffin-embedded, formalin-fixed tumour sections from vector- and N714 clone-derived tumours. Ki-67 was detected within the nuclei by brown stain. Haematoxylin was used for counterstaining. (B) Apoptotic cells were detected in the tumour sections by TUNEL staining. Formalin-fixed paraffin-embedded tumour (2-week post-implant) sections were de-paraffinised, hydrated and treated with proteinase K and H_2O_2. Then tissue sections were stained using a TUNEL assay kit. Apoptotic cells showed brown colour and counterstaining was performed with methyl green. Left panel includes representative fields from the control group consisting of sections from vector-derived and parental cell-derived tumours. Right panel shows representative fields from sections of DN-Stat3-expressing clone-derived tumours. (C) Quantification of apoptotic cells was presented as the percentage (mean ± SEM, $n = 3$) of TUNEL-positive cells in three random fields of each tumour of week 2 post-tumour implantation.

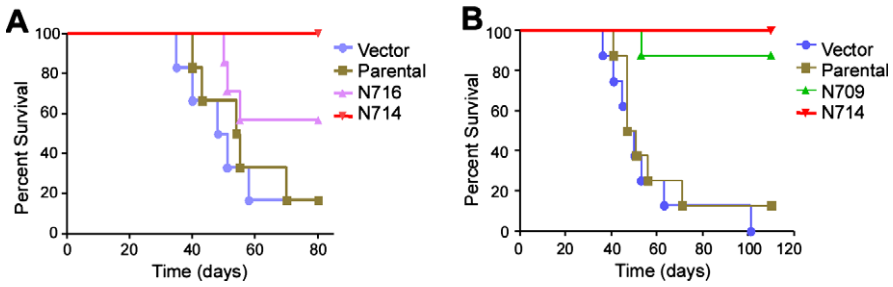

Fig. 5 – DN-Stat3 prolongs the survival of mice with orthotopically implanted tumour. Kaplan–Meier curves represent survival of mice that were orthotopically implanted with U87-derived clones. (A) Vector, parental, N714 and N716 (n = 6 for each group), and (B) vector, parental, N709 and N714 (n = 8 for each group).

control groups died within 7 weeks after tumour implantation, 100% of the N709 and N714 survived longer. Mice implanted with N716 clone showed 50% survival within this time period. These data correlate to the tumour progression observed by the increase in tumour volume in flanks (Fig. 2). Taken together, these results suggest that activated Stat3 plays an essential role in the tumourigenesis and progression of U87 cell-derived tumour growth in immune-compromised mice.

3.5. *Neo-angiogenesis is compromised in DN-Stat3-expressing U87-derived tumours in immune-compromised mice*

The results described above indicate that activated Stat3 is required for the progression of U87-derived tumour growth in immune-compromised mice. GBM outgrowth (>2 mm in diameter or thickness) is associated with hypoxia, necrosis and neo-angiogenesis,[13,28] and hypoxia is a primary inducer of angiogenesis.[16–18,29] In GBM, VEGF and IL-8 produced by hypoxic tumour cells serve as the major pro-angiogenic factors.[13,19] Stat3 has been shown to be a transcriptional regulator of the *VEGF* gene in melanoma, renal cell carcinoma and breast cancer cells.[20,21,30] Therefore, to test the hypothesis that activated Stat3 is also required for the induction of neo-angiogenesis in GBM, we measured the effects of DN-Stat3 expression on *VEGF* promoter activity by using 2.274 kb human *VEGF* promoter-driven luciferase construct[31] and endogenous *VEGF* mRNA expression by real-time PCR, in U87 cells under hypoxia (48 h). The results revealed that DN-Stat3 significantly reduced hypoxia-induced *VEGF* promoter activity (Fig. 6A) and the *VEGF* mRNA expression (Fig. 6B). Next, to examine if Stat3 activation was involved in the induction of neo-angiogenesis in U87 cell line-derived tumours, we stained tumour sections for CD105. CD105, also known as endoglin, is a proliferation-associated and hypox-

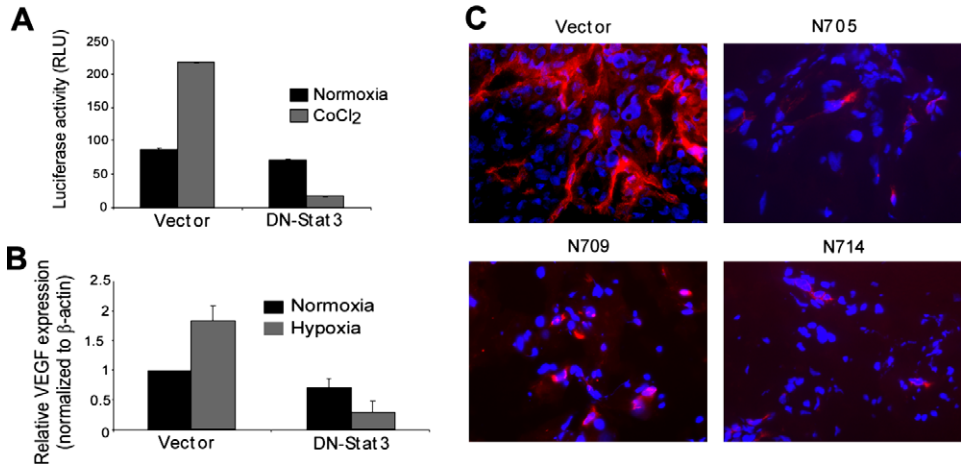

Fig. 6 – DN-Stat3 compromises neo-angiogenesis in GBM. (A) DN-Stat3 inhibits the *VEGF* promoter-driven luciferase activity in hypoxic U87 cells *in vitro*. Cells were co-transfected with a luciferase construct (2.274 kb human *VEGF* promoter cloned in the promoter-less luciferase expression vector, pGL3-basic) and DN-Stat3 expression plasmid. Twenty-four hour post-transfection cells were exposed to 1.4% O_2 (hypoxia) or normoxia for 48 h. Derived cell extracts were subjected to luciferase assays and results were normalised. Each value of luciferase activity represents mean ± SEM of three independent determinations. (B) DN-Stat3 reduces the steady state level of *VEGF* mRNA in hypoxic U87 cells. Values are normalised against the β-actin level and the ratio to basal *VEGF* level under normoxia is shown in each case. (C) New blood vessel formation is compromised in DN-Stat3-expressing tumours. Frozen, acetone-fixed tumour sections were stained with anti-CD105 antibody followed by staining with Alexa Fluor 595, washed and mounted with Vectashield containing DAPI. Newly formed blood vessels were stained with red fluorescence, whereas nuclei were stained blue.

ia-inducible protein abundantly expressed on the surface of angiogenic endothelial cells.[32] Our immunostaining experiments with anti-CD105 antibody revealed the presence of large and abundant newly formed blood vessels in the tumours derived from vector control U87cells, whereas almost none or very few incomplete vessels were seen in the DN-Stat3-expressing U87 clone-derived tumours (Fig. 6C). These results show that neo-angiogenesis was inhibited in DN-Stat3-expressing tumours, probably leading to cell death, as shown by TUNEL assay (Fig. 4).

4. Discussion

We have previously shown that in the GBM cell line U87, Stat3 is activated by EGFR and that activated Stat3 suppresses the spontaneous apoptosis of U87 cells by upregulating the expression of the pro-survival protein Mcl-1 *in vitro*.[9] In U87 cells, although the EGFR-activated PI3K-AKT pathway significantly contributes to the cell survival, Stat3 activation is critical for the suppression of spontaneous apoptosis *in vitro*.[9] To define the role of constitutively activated Stat3 in the growth of GBM *in vivo*, we generated stable U87-derived clones expressing DN-Stat3 under a constitutive CMV-promoter.[9] The constitutive DN-Stat3-expressing U87 cells-derived tumours grown in flanks of nude mice were significantly smaller than those derived from the parental or vector control cells (data not shown). Although this finding has suggested that activated Stat3 plays a role in the growth of U87 cell-derived tumours, further evaluation of Stat3 function in the pathogenesis of GBM becomes difficult due to the instability of the U87-derived clones that constitutively express the DN-Stat3 protein.

We have overcome this difficulty by expressing DN-Stat3 both *in vitro* and *in vivo* in U87 GBM cell line in a hypoxia/HIF-1-inducible manner. Using this expression system, we made the important observations that DN-Stat3 dramatically reduced U87 clone-derived tumour growth in mice by inhibiting the proliferation and survival of tumour cells, and more importantly, by suppressing tumour neo-angiogenesis. Thus, we have clearly demonstrated by using a widely used model tumourigenic GBM cell line U87 and rodent xenograft brain tumour model that activated Stat3 was required for the growth of human GBM. Our findings emphasise the significance of the persistent activation of Stat3 in more than 90% of GBM tumours and all GBM cell lines examined.[7–9]

In GBM cells, Stat3 can be activated by multiple cytokine- and growth factor-signalling pathways including IL-4, IL-6 and EGF.[7,10,12] Under normal physiological conditions, Stat3 activation is limited in both magnitude and duration.[12] However, Stat3 activation is persistent in a variety of other human malignancies.[11] It has been elegantly demonstrated by Bromberg and colleague that a genetically engineered, constitutively active Stat3 is capable of inducing cellular transformation and tumour formation in nude mice.[33] Therefore, targeting Stat3 could be a promising strategy to fight GBM and other human malignancies in which persistently activated Stat3 contributes to the pathogenesis of the disease. Of note, deletion of *stat3* in mice, unlike six other *stat* genes, results in embryonic lethality.[34,35] Therefore, anti-Stat3 therapy in cancers such as GBM should be target-specific, minimising the off-target detrimental effects of Stat3 inhibitors on normal cells.

The brain is a highly vascularised organ in which normal cells are normoxic, whereas the GBM cells in the tumour become hypoxic due to occlusion of the existing blood vessels.[13] Therefore, expression of DN-Stat3 through a hypoxia-inducible expression vector is a novel approach to target GBM cells *in vivo*. In principle, blockade of Stat3 activation in GBM cells by DN-Stat3 would restrain them from activating the angiogenic switch, thereby halting the tumour growth and maintaining the tumour dormancy. We have proven this principle by demonstrating that intracranial implants of hypoxia-inducible DN-Stat3-expressing U87 clones failed to kill mice, whereas 80% of vector control or parental U87 cell-implanted mice died within 2 months. Further studies expressing DN-Stat3 using this hypoxia-inducible vector in other tumourigenic GBM cell lines are necessary to confirm that Stat3 activation in hypoxic GBM cells plays an indispensable role in activating the angiogenic switch.

Conflict of interest statement

None declared.

Acknowledgements

We thank Drs. Janet Houghton, Gene Barnett, Serpil Erzurum, Pankaj Sharma, Fred Hsieh and Robert Weil for critical comments, Phyllis Harbor and Saroja N. Devi for technical assistance and Dr. Judith Drazba and Rikhia Chakraborty for assistance in imaging. This work was supported by Grants R01CA095006 and R01CA116804 from the National Institutes of Health to SJH and EGVM, respectively.

Appendix A. Supplementary material

Supplementary data associated with this article can be found, in the online version, at doi:10.1016/j.ejca.2008.11.027.

REFERENCES

1. Maher EA, Furnari FB, Bachoo RM, et al. Malignant glioma: genetics and biology of a grave matter. *Genes Dev* 2001;**15**(11):1311–33.
2. Ohgaki H, Kleihues P. Epidemiology and etiology of gliomas. *Acta Neuropathol (Berl)* 2005;**109**(1):93–108.
3. Holland EC. Glioblastoma multiforme: the terminator. *Proc Natl Acad Sci USA* 2000;**97**(12):6242–4.
4. Wechsler-Reya R, Scott MP. The developmental biology of brain tumors. *Ann Rev Neurosci* 2001;**24**:385–428.
5. McLendon R, Friedman A, Bigner D, et al. Comprehensive genomic characterization defines human glioblastoma genes and core pathways. *Nature* 2008.
6. Parsons DW, Jones S, Zhang X, et al. An integrated genomic analysis of human glioblastoma multiforme. *Science* 2008;**321**(5897):1807–12.
7. Rahaman SO, Harbor PC, Chernova O, et al. Inhibition of constitutively active Stat3 suppresses proliferation and

induces apoptosis in glioblastoma multiforme cells. *Oncogene* 2002;**21**(55):8404–13.
8. Rahaman SO, Vogelbaum MA, Haque SJ. Aberrant Stat3 signaling by interleukin-4 in malignant glioma cells: involvement of IL-13Ralpha2. *Cancer Res* 2005;**65**(7):2956–63.
9. Ghosh MK, Sharma P, Harbor PC, Rahaman SO, Haque SJ. PI3K-AKT pathway negatively controls EGFR-dependent DNA-binding activity of Stat3 in glioblastoma multiforme cells. *Oncogene* 2005;**24**(49):7290–300.
10. Zhong Z, Wen Z, Darnell Jr JE. Stat3: a STAT family member activated by tyrosine phosphorylation in response to epidermal growth factor and interleukin-6. *Science* 1994;**264**(5155):95–8.
11. Yu H, Jove R. The STATs of cancer – new molecular targets come of age. *Nat Rev Cancer* 2004;**4**(2):97–105.
12. Haque SJ, Sharma P. Interleukins and STAT Signaling. *Vitam Horm* 2006;**74C**:165–206.
13. Brat DJ, Van Meir EG. Vaso-occlusive and prothrombotic mechanisms associated with tumor hypoxia, necrosis, and accelerated growth in glioblastoma. *Lab Invest* 2004;**84**(4):397–405.
14. Bao S, Wu Q, Sathornsumetee S, et al. Stem cell-like glioma cells promote tumor angiogenesis through vascular endothelial growth factor. *Cancer Res* 2006;**66**(16):7843–8.
15. Gimbrone Jr MA, Leapman SB, Cotran RS, Folkman J. Tumor dormancy in vivo by prevention of neovascularization. *J Exp Med* 1972;**136**(2):261–76.
16. Folkman J. Angiogenesis. *Ann Rev Med* 2006;**57**:1–18.
17. Naumov GN, Bender E, Zurakowski D, et al. A model of human tumor dormancy: an angiogenic switch from the nonangiogenic phenotype. *J Natl Cancer Inst* 2006;**98**(5):316–25.
18. Harris AL. Hypoxia – a key regulatory factor in tumour growth. *Nat Rev Cancer* 2002;**2**(1):38–47.
19. Brat DJ, Castellano-Sanchez A, Kaur B, Van Meir EG. Genetic and biologic progression in astrocytomas and their relation to angiogenic dysregulation. *Adv Anat Pathol* 2002;**9**(1):24–36.
20. Jung JE, Lee HG, Cho IH, et al. STAT3 is a potential modulator of HIF-1-mediated VEGF expression in human renal carcinoma cells. *Faseb J* 2005;**19**(10):1296–8.
21. Niu G, Wright KL, Huang M, et al. Constitutive Stat3 activity up-regulates VEGF expression and tumor angiogenesis. *Oncogene* 2002;**21**(13):2000–8.
22. Kaptein A, Paillard V, Saunders M. Dominant negative stat3 mutant inhibits interleukin-6-induced Jak-STAT signal transduction. *J Biol Chem* 1996;**271**(11):5961–4.
23. Post DE, Van Meir EG. Generation of bidirectional hypoxia/HIF-responsive expression vectors to target gene expression to hypoxic cells. *Gene Ther* 2001;**8**(23):1801–7.
24. Haque SJ, Harbor PC, Williams BR. Identification of critical residues required for suppressor of cytokine signaling-specific regulation of interleukin-4 signaling. *J Biol Chem* 2000;**275**(34):26500–6.
25. Haque SJ, Wu Q, Kammer W, et al. Receptor-associated constitutive protein tyrosine phosphatase activity controls the kinase function of JAK1. *Proc Natl Acad Sci USA* 1997;**94**(16):8563–8.
26. Attia MA, Weiss DW. Immunology of spontaneous mammary carcinomas in mice. V. Acquired tumor resistance and enhancement in strain A mice infected with mammary tumor virus. *Cancer Res* 1966;**26**(8):1787–800.
27. Wang G, Hazra TK, Mitra S, Lee HM, Englander EW. Mitochondrial DNA damage and a hypoxic response are induced by CoCl(2) in rat neuronal PC12 cells. *Nucl Acid Res* 2000;**28**(10):2135–40.
28. Rong Y, Durden DL, Van Meir EG, Brat DJ. 'Pseudopalisading' necrosis in glioblastoma: a familiar morphologic feature that links vascular pathology, hypoxia, and angiogenesis. *J Neuropathol Exp Neurol* 2006;**65**(6):529–39.
29. Bergers G, Benjamin LE. Tumorigenesis and the angiogenic switch. *Nat Rev Cancer* 2003;**3**(6):401–10.
30. Comhair SA, Xu W, Ghosh S, et al. Superoxide dismutase inactivation in pathophysiology of asthmatic airway remodeling and reactivity. *Am J Pathol* 2005;**166**(3):663–74.
31. Shi Q, Le X, Abbruzzese JL, et al. Constitutive Sp1 activity is essential for differential constitutive expression of vascular endothelial growth factor in human pancreatic adenocarcinoma. *Cancer Res* 2001;**61**(10):4143–54.
32. Duff SE, Li C, Garland JM, Kumar S. CD105 is important for angiogenesis: evidence and potential applications. *Faseb J* 2003;**17**(9):984–92.
33. Bromberg JF, Wrzeszczynska MH, Devgan G, et al. Stat3 as an oncogene. *Cell* 1999;**98**(3):295–303.
34. Takeda K, Noguchi K, Shi W, et al. Targeted disruption of the mouse Stat3 gene leads to early embryonic lethality. *Proc Natl Acad Sci USA* 1997;**94**(8):3801–4.
35. Levy DE, Lee CK. What does Stat3 do? *J Clin Invest* 2002;**109**(9):1143–8.